2015 IEEE 54th Annual Conference on Decision and Control (CDC)
December 15-18, 2015. Osaka, Japan

# Torwards Uncertainty Optimization in Active SLAM

Pedro Lourenço, Pedro Batista, Paulo Oliveira, and Carlos Silvestre

*Abstract*— **This paper addresses the problem of optimizing the uncertainty in an active simultaneous localization and mapping algorithm. This is done by designing an optimization problem that weighs the final uncertainty, the average uncertainty in the horizon considered, and the cost of the control. Using the Pontryagin minimum principle and building on [1] and [2], the optimization problem is transformed into a two-point boundary value problem that encodes necessary conditions for the input that minimizes the uncertainty. The problem is solved numerically, and several particular examples are analysed in depth.**

## I. Introduction

Simultaneous localization and mapping (SLAM) is the problem of navigating a vehicle in an unknown environment, by building a map of the area and using this map to deduce its location, without the need for *a priori* knowledge of location. Research efforts on this problem are interestingly and thoroughly reported in the survey on SLAM techniques found in [3]. The main paradigm in SLAM is to move to gain new knowledge and improve what is known. In the formative years of SLAM, the question of how to move was completely separated from the estimation problem. However, in recent years, several works addressed the issue of intelligent moving in the context of SLAM, thus introducing Active SLAM (see [4] and [5]).

The objective of Active SLAM is to plan ahead the motion of the vehicle in order to maximize the explored areas and minimize the uncertainty associated with the estimation. These two objectives are, in a sense, complementary: exploration involves moving in previously unvisited terrain with the objective of increasing the overall knowledge of the environment, while the latter is exploitation, i.e., it involves revisiting areas to maximize the information gain. In this paper, the focus is on the exploitation part of Active SLAM, which requires that some form of exploration is already done.

One of the main discussions in the optimization of the exploitation step is how to measure uncertainty, or better, how to quantify the information gain [6]. The main possibilities, stemming from the EKF approach to SLAM [7], are 1) *A-opt* - the trace of the covariance, i.e., the average variance across all states; 2) *D-opt* - the determinant of the covariance, which is proportional to the volume of the covariance matrix; 3) *E-opt* - the minimum eigenvalue of the covariance; and 4) the entropy of the distribution. In [6] a comparison of these uncertainty criteria with planning under uncertainty is provided, concluding that *D-opt* is, in their case, the one with best results, even though most of the literature in Active SLAM utilizes the A-opt criterion. The most relevant issue in Active SLAM is, however, how to find the path that minimizes the uncertainty. One possibility is to address this as the problem of planning the sequence of discrete positions through the environment that form the maximally informative trajectory, by discretizing the environment into a grid, as is done in [8] for EKF-SLAM and in [9] for particle filter SLAM. Another approach [10] follows the recent trend of multiple robot missions and uses relative entropy optimization and an EKF.

Not specifically applied to Active SLAM, but still with the objective of uncertainty reduction, an interesting idea is proposed in [2]. The author recovers a traditional optimal control and estimation result [1], and, using the Pontryagin minimum principle [11], derives a control strategy for mobile sensors that influences the uncertainty evolution in a Kalman filter. Given the linear character of the Kalman filter, this is only possible if one or more of the parameters of the filter depends, even if indirectly, on the input of another system.

This paper is rooted on this idea and on previous results in SLAM where the problem was addressed in a sensor-based framework [12] resulting, within certain conditions, in a linear time-varying Kalman filter with globally exponentially stable (GES) error dynamics. The cost functional proposed in [2] is used to define an optimization problem for a more general class of systems into which the sensor-based SLAM framework fits, and the Pontryagin minimum principle is used in a similar way. The main contributions of this paper are the extension of the idea in [2] to a more general class of systems, and the proposal of necessary conditions for the trajectory that optimizes the uncertainty in a SLAM Kalman filter. These conditions appear in the form of a two-point boundary value problem that is solved numerically, and some examples are analysed in depth.

The paper is organized as follows. Section II overviews the sensor-based SLAM approach and presents the problem statement. In Section III the ideas on which this paper builds are reviewed, and a control strategy for uncertainty reduction through optimal motion planning is presented. Section IV applies the previous results to active SLAM. Numerical results are presented and discussed in Section V, followed by conclusions and future work directions in Section VI.

This work was supported by the Fundação para a Ciência e a Tecnologia (FCT) through ISR under LARSyS UID/EEA/50009/2013, and through IDMEC, under LAETA UID/EMS/50022/2013 contracts, by the University of Macau Project MYRG2015-00126-FST, and by the Macao Science and Technology Development Fund under Grant FDCT/048/2014/A1. The work of P. Lourenço was supported by the PhD. Student Grant SFRH/BD/89337/2012 from FCT.

The authors are with the Institute for Systems and Robotics, Laboratory of Robotics and Systems in Engineering and Practice, Portugal. P. Batista is also with Instituto Superior Técnico, Universidade de Lisboa, Portugal. P. Oliveira is also with the Department of Mechanical Engineering, Instituto Superior Técnico, Universidade de Lisboa, Portugal. C. Silvestre is with the Department of Electrical and Computer Engineering of the Faculty of Science and Technology of the University of Macau, Macao, China, on leave from Instituto Superior Técnico, Universidade de Lisboa, Lisbon, Portugal.
{plourenco,pbatista,pjcro}@isr.ist.utl.pt, csilvestre@umac.mo

*Notation:* Throughout this paper, $\mathbf{I}_n$ is the identity matrix of dimension $n$, $\mathbf{0}_{n\times m}$ is a $n$ by $m$ matrix filled with zeros, and $\mathbf{1}_i \in \mathbb{R}^n$ is a vector whose only nonzero entry (equal to 1) is the $i$-th one. $\mathbf{S}(\mathbf{a})$ is a skew-symmetric matrix that encodes the cross-product. Quantities denoted with $(.)\big|_*$ are evaluated along the optimal trajectory.

## II. Sensor-based SLAM Overview

Building on the idea of robocentric filtering, [13] and [12] address the problem of designing a navigation system in a sensor-based framework for a vehicle capable of sensing landmarks in a previously unknown environment, in 2-D and 3-D respectively. This is done resorting to a purely sensor-based SLAM algorithm where no linearization or approximation is used whatsoever and pose representation in the state is suppressed, therefore avoiding its pitfalls. This section presents a brief overview of the work proposed in those papers, that serve as groundwork for the optimal control problem to address in this work.

### A. Nonlinear system dynamics

Let the pair $\left(\mathbf{R}(t), {}^I\mathbf{p}(t)\right) \in \mathrm{SO}(n) \times \mathbb{R}^n$, $n = \{2, 3\}$, encode the transformation from the body-fixed frame $\{B\}$ to an inertial frame $\{I\}$. $\mathbf{R}(t)$ is a rotation matrix satisfying $\dot{\mathbf{R}}(t) = \mathbf{R}(t)\mathbf{S}(\boldsymbol{\omega}(t))$, where $\boldsymbol{\omega}(t) \in \mathbb{R}^{\frac{n(n-1)}{2}}$ is the angular velocity, expressed in body-fixed coordinates, and ${}^I\mathbf{p}(t)$ represents the vehicle position, assumed coincident with the origin of the body-fixed frame, in the inertial frame. Consider also the existence of static landmarks in the environment whose coordinates can be perceived by the vehicle. These define the map and can be separated in two complementary sets, $\mathcal{M}_O$ and $\mathcal{M}_U$. The former contains the $m_O$ visible landmarks, while the latter contains the $m_U$ non-visible.

Consider that the vehicle is equipped with a triad of orthogonally mounted rate gyros, rendering the angular velocity of the vehicle available through the biased rate gyros measurements $\boldsymbol{\omega}_m(t) = \boldsymbol{\omega}(t) + \mathbf{b}_\omega(t)$, where the bias $\mathbf{b}_\omega(t) \in \mathbb{R}^{\frac{n(n-1)}{2}}$ is assumed constant and unknown. Taking this into account, it is possible to assemble the system

$$\begin{cases} \dot{\mathbf{p}}_i(t) = -\mathbf{S}(\boldsymbol{\omega}(t))\,\mathbf{p}_i(t) - \mathbf{v}(t),\ \forall i \in \mathcal{M} \\ \dot{\mathbf{b}}_\omega(t) = \mathbf{0} \\ \mathbf{y}_i(t) = \mathbf{p}_i(t), \forall i \in \mathcal{M}_O \\ \boldsymbol{\omega}_m(t) = \boldsymbol{\omega}(t) + \mathbf{b}_\omega(t) \end{cases}, \qquad (1)$$

where $\mathbf{p}_i(t) \in \mathbb{R}^n$ is the position of a landmark and $\mathbf{v}(t) \in \mathbb{R}^n$ is the velocity of the vehicle, both expressed in the body-fixed frame. The last two quantities are measured. This system can be transformed to incorporate $\boldsymbol{\omega}_m(t)$ in the dynamics of the landmarks, using the property $\mathbf{S}(\mathbf{a})\mathbf{b} = \bar{\mathbf{S}}^T(\mathbf{b})\,\mathbf{a}$, where $\bar{\mathbf{S}}^T(\mathbf{b})$ is equal to $\mathbf{S}(1)\mathbf{b}$ or $-\mathbf{S}(\mathbf{b})$, for $n = 2$ or $n = 3$, respectively.

The linear velocity and the angular measurement bias constitute the vehicle state, denoted by $\mathbf{x}_V(t) := \begin{bmatrix}\mathbf{v}^T(t) & \mathbf{b}_\omega^T(t)\end{bmatrix}^T \in \mathbb{R}^{n_V}$. Both are assumed, in a deterministic setting, as constant. In the adopted filtering framework, however, the inclusion of state disturbances allows to consider them as slowly time-varying. The landmarks in each set can be stacked in state vectors denoted as $\mathbf{x}_{O_i}(t) = \mathbf{p}_i(t)$, $i \in \mathcal{M}_O$ and $\mathbf{x}_{U_i}(t) = \mathbf{p}_i(t)$, $i \in \mathcal{M}_U$, which together form the landmark state vector $\mathbf{x}_M(t) = \begin{bmatrix}\mathbf{x}_O^T(t) & \mathbf{x}_U^T(t)\end{bmatrix}^T \in \mathbb{R}^{n_O+n_U}$. This is the framework derived in [12] for the sensor-based simultaneous localization and mapping algorithm proposed therein to estimate the map, the angular velocity bias, and the linear velocity of the vehicle. However, in this paper the linear velocity will act as an input and therefore will not be present in the full system state, $\mathbf{x}_T(t) = \begin{bmatrix}\mathbf{b}_\omega^T(t) & \mathbf{x}_M^T(t)\end{bmatrix}^T$. The full input vector is $\mathbf{u}(t) = \begin{bmatrix}\mathbf{v}^T(t) & \boldsymbol{\omega}^T(t)\end{bmatrix}^T$, with the full system dynamics reading as

$$\begin{cases} \dot{\mathbf{x}}_T(t) = \mathbf{A}_T(\mathbf{y}(t), \mathbf{x}_U(t), \mathbf{u}(t))\mathbf{x}_T(t) + \mathbf{B}_T\mathbf{v}(t) \\ \mathbf{y}(t) = \mathbf{x}_O(t) \end{cases}, \qquad (2)$$

with

$$\mathbf{A}_T(\mathbf{y}(t), \mathbf{x}_U(t), \mathbf{u}(t)) = \begin{bmatrix} \mathbf{0}_{n_V} & \mathbf{0}_{n_V\times n_M} \\ \mathbf{A}_{MV}(\mathbf{y}(t), \mathbf{x}_M(t)) & \mathbf{A}_M(\mathbf{u}(t)) \end{bmatrix},$$

and $\mathbf{B}_T = \begin{bmatrix}\mathbf{0}_{n\times\frac{1}{2}n(n-1)} & \mathbf{I}_n & \cdots & \mathbf{I}_n\end{bmatrix}^T$, where

$$\mathbf{A}_{MV}(\mathbf{y}(t), \mathbf{x}_U(t)) = \begin{bmatrix}\bar{\mathbf{S}}(\mathbf{p}_1(t)) & \cdots & \bar{\mathbf{S}}(\mathbf{p}_m(t))\end{bmatrix}^T$$

and $\mathbf{A}_M(\mathbf{u}(t)) = \operatorname{diag}\left(-\mathbf{S}(\boldsymbol{\omega}_m(t)), \cdots, -\mathbf{S}(\boldsymbol{\omega}_m(t))\right)$. From (2) it follows that the system may be expressed in a way similar to the usual linear system form. However, it can be seen that the system above is nonlinear, as the dynamics matrix depends on the landmarks that constitute the state, as well as on the input. On the other hand, it must be noted that, as $\mathbf{y}(t) = \mathbf{x}_O(t)$, the dynamics matrix can be written as a function of the system output and the non-visible landmarks.

### B. System observability and observer convergence

In [13] and [12], the version of system (2) with the velocity as part of the state is studied for observability purposes and conditions for its observability and uniform complete observability are found. These include, for example, the existence of two landmarks (2-D) or three landmarks that define a plane (3-D) as sufficient conditions. The observability analysis leads towards the design of a state observer, such as the linear time-varying (LTV) Kalman filter, with globally exponentially stable error dynamics. It is shown also that this observer doubles as an observer for the nominal nonlinear system (1) while converging exponentially to the true state.

In those works, the linear velocity was one of the states not directly observed (the rate-gyro bias being the other). Now, the linear velocity is an input, and therefore the observability restrictions are lightened. This is done to let the definition of the trajectory of the vehicle free, depending upon a control strategy which provides linear and angular velocities.

### C. Problem Statement

The problem considered in this paper is to find a control strategy that provides $\mathbf{v}(t)$ and $\boldsymbol{\omega}(t)$ such that the uncertainty in the Kalman filters derived in [13] and [12] is optimized, i..e, it is reduced to a minimum. This fits under the problem of active simultaneous localization and mapping, i.e., optimal motion planning to reduce the uncertainty on the estimates.

## III. Optimal Motion Planning for Uncertainty Reduction

In this section, the problem of optimal motion planning for uncertainty reduction is tackled by means of the Pontryagin Minimum Principle (PMP) for cost functionals with fixed time, free endpoint, and terminal cost. The following subsection addresses this issue.

## A. The Pontryagin Minimum Principle

The PMP [11, Theorem 5-11] is a very powerful and elegant result in the field of optimal control, even though it only establishes necessary conditions for the optimality of a control law, as it transforms a potentially cumbersome optimization problem into an ordinary differential equation with two-point boundary conditions, provided that a minimum for the Hamiltonian is found. This result applies for a very general class of systems that can be driven by an input. Its best known application is the linear case with a quadratic cost, better known as the linear quadratic regulator (LQR) [11]. However, it can also be applied to optimal estimation, as advanced in [1]. The Kalman filter can be derived using the PMP and a terminal cost functional depending on the trace of the filter covariance. This is done by defining a matrix costate $\mathbf{\Lambda}(t)$ whose elements serve as costates for the elements of the filter covariance, and, through the PMP, finding the "control", i.e., the filter gain, that minimizes the trace of the covariance weighted by some matrix $\boldsymbol{\mathcal{M}}$. Based on the innovative approach proposed by Athans in [1], Hussein [2] proposed a filter for linear systems where the covariance of the measurement noise $\mathbf{R}$ depends upon the state of an underlying linear dynamical system. There he combined the derivation of the Kalman filter found in [1] with the traditional optimal control formulation, by using the input of the underlying system as another degree-of-freedom (along with the Kalman gain). To solve the problem, a new costate $\boldsymbol{\lambda}(t)$ is added as a counterpart for the dynamics of the underlying system, and the PMP is used to provide necessary conditions for the optimal state trajectory of the underlying nonlinear system that minimizes the filter covariance. This results in the cost functional

$$J(\mathbf{u}) = \operatorname{tr}\left(\boldsymbol{\mathcal{M}}\mathbf{P}(t_f)\right) + \int_{t_0}^{t_f} \left( \frac{1}{2}\mathbf{u}^T(t)\boldsymbol{\mathcal{R}}\mathbf{u}(t) + \operatorname{tr}\left(\boldsymbol{\mathcal{Q}}\mathbf{P}(t)\right) \right) \mathrm{d}t \tag{3}$$

where $\boldsymbol{\mathcal{R}}$, $\boldsymbol{\mathcal{Q}}$, and $\boldsymbol{\mathcal{M}}$ are all positive-definite matrices. The control problem at hand is to find an admissible function $\mathbf{u} \in \mathbb{R}^{n_u}$ that minimizes this cost functional, i.e.,

$$\mathbf{u}^*(t) = \arg\min_{\mathbf{u}(t)} J(\mathbf{x}(t_0), \mathbf{P}(t_0), t_0, \mathbf{u}(t))$$

subject to the dynamics of the covariance and of the underlying system. For this problem, Hussein proposes the Hamiltonian

$$H(\mathbf{P}(t), \mathbf{x}(t), \boldsymbol{\lambda}(t), \mathbf{\Lambda}(t), \mathbf{u}(t)) = \operatorname{tr}\left(\Lambda^T(t)\dot{\mathbf{P}}(t)\right) + \boldsymbol{\lambda}^T(t)\dot{\mathbf{x}}(t) + \frac{1}{2}\mathbf{u}^T(t)\boldsymbol{\mathcal{R}}\mathbf{u}(t) + \operatorname{tr}\left(\boldsymbol{\mathcal{Q}}\mathbf{P}(t)\right),$$

and using the PMP he manages to solve the sufficient conditions for minimization of a scalar field $H(\mathbf{u})$ [14, Theorem 2.4],

$$\boldsymbol{\nabla}_{\mathbf{u}} H(\mathbf{u}(t))\big|_* = 0 \quad \text{and} \quad \frac{\partial^2}{\partial\mathbf{u}\partial\mathbf{u}^T} H(\mathbf{u}(t))\big|_* \succ \mathbf{0},$$

analytically and to find expressions for the costates.

In this section, we propose a control strategy that applies to a special kind of systems that can be related to the problem introduced above. In order to lighten the notation, the dependence on time of all the variables will be left implicit except when it is evaluated in a particular time instant.

## B. Control strategy for a class of nonlinear systems

Let $\mathbf{x}(t) \in \mathbb{R}^n$ be the state of a system with nonlinear dynamics

$$\begin{cases} \dot{\mathbf{x}} = \mathbf{f}(\mathbf{x}, \mathbf{u}) \\ \mathbf{y} = \mathbf{h}(\mathbf{x}, \mathbf{u}) \end{cases}, \tag{4}$$

where $\mathbf{f}(\mathbf{x}, \mathbf{u})$ can be written as $\mathbf{f}(\mathbf{x}, \mathbf{u}) = \mathbf{A}(\mathbf{x}, \mathbf{u})\mathbf{x} + \mathbf{B}(\mathbf{x}, \mathbf{u})\mathbf{u}$. Suppose that this system accepts a transformation $(\mathbf{x}_T, \mathbf{y}_T) = \mathbf{T}(\mathbf{x}, \mathbf{y}) \in \mathbb{R}^{n_T} \times \mathbb{R}^{n_{y_T}}$ that results in a system affine in its state that can be regarded as LTV

$$\begin{cases} \dot{\mathbf{x}}_T = \mathbf{A}_T(\mathbf{y}, \mathbf{u})\mathbf{x}_T + \mathbf{B}_T(\mathbf{y}, \mathbf{u})\mathbf{u} \\ \mathbf{y}_T = \mathbf{C}_T(\mathbf{y}, \mathbf{u})\mathbf{x}_T \end{cases}, \tag{5}$$

and whose dynamics mimic the dynamics of (4). If conditions for the uniform complete observability of the pair $(\mathbf{A}_T(\mathbf{y}, \mathbf{u}), \mathbf{C}_T(\mathbf{y}, \mathbf{u}))$ are verified, then a Kalman filter can be designed for system (5) with GES error dynamics [15]. Furthermore, the transformation $\mathbf{T}(\mathbf{x}, \mathbf{y})$ is assumed to respect the conditions in [16], and, as such, this observer can also be used as an observer for the nonlinear system (4). Adding perturbation noise to both the dynamics and the output equations in (5), and denoting as $\mathbf{P}(t) \in \mathbb{R}^{n_T \times n_T}$ the covariance of the estimation error of $\mathbf{x}_T$, $\mathbf{Q}$ as the covariance of the perturbed version of (5), and $\mathbf{R}(\mathbf{y}, \mathbf{u})$ as the covariance of the perturbed output $\mathbf{y}_T$ that may depend on the input and output of the system, the observer dynamics are

$$\begin{aligned} \dot{\mathbf{P}} = {} & \mathbf{A}_T(\mathbf{y}, \mathbf{u})\mathbf{P} + \mathbf{P}\mathbf{A}_T^T(\mathbf{y}, \mathbf{u}) + \mathbf{Q} \\ & - \mathbf{P}\mathbf{C}_T^T(\mathbf{y}, \mathbf{u})\mathbf{R}^{-1}(\mathbf{y}, \mathbf{u})\mathbf{C}_T(\mathbf{y}, \mathbf{u})\mathbf{P}. \end{aligned} \tag{6}$$

As the observer dynamics depend on the input and output of the system to be estimated, different inputs (which may lead to a diversity of outputs) will induce different levels of uncertainty in the estimation. The following results address this issue.

*Theorem 1:* Let $\mathbf{u}^*(t)$ be an admissible control which transfers $(\mathbf{x}_0, \mathbf{P}_0, t_0)$ to the target set $\mathbb{R}^{n_x} \times \mathbb{R}^{n_T \times n_T} \times \{t_f\}$. Let $\mathbf{x}^*(t)$ and $\mathbf{P}^*(t_0)$ be the trajectories of (4) and (6) corresponding to $\mathbf{u}^*(t)$, originating at $(\mathbf{x}_0, \mathbf{P}_0, t_0)$ and meeting the target set at $t_f$. If $\mathbf{u}^*(t)$ is optimal for the cost functional (3), then it is necessary that there exist functions $\boldsymbol{\lambda}^*(t)$ and $\mathbf{\Lambda}^*(t)$ such that:

(i) the vector costate $\boldsymbol{\lambda}^*(t)$ satisfies

$$\begin{aligned} \dot{\boldsymbol{\lambda}} = {} & -\mathbf{A}^T\boldsymbol{\lambda} - \mathbf{g}\left(\mathbf{x}\boldsymbol{\lambda}^T, \frac{\partial\mathbf{A}}{\partial\mathbf{x}}\right) - \mathbf{g}\left(\mathbf{u}\boldsymbol{\lambda}^T, \frac{\partial\mathbf{B}}{\partial\mathbf{x}}\right) \\ & - \mathbf{g}\left(\mathbf{P}(\mathbf{\Lambda} + \mathbf{\Lambda}^T), \frac{\partial\mathbf{A}_T}{\partial\mathbf{x}}\right) \\ & + \mathbf{g}\left(\mathbf{P}(\mathbf{\Lambda} + \mathbf{\Lambda}^T)\mathbf{P}\mathbf{C}_T^T\mathbf{R}^{-1}, \frac{\partial\mathbf{C}_T}{\partial\mathbf{x}}\right) \\ & - \mathbf{g}\left(\mathbf{R}^{-1}\mathbf{C}_T\mathbf{P}\mathbf{\Lambda}\mathbf{P}\mathbf{C}_T^T\mathbf{R}^{-1}, \frac{\partial\mathbf{R}}{\partial\mathbf{x}}\right) \end{aligned}$$

with boundary condition $\boldsymbol{\lambda}(t_f) = \mathbf{0}$;

(ii) the matrix costate $\mathbf{\Lambda}^*(t)$ associated with the covariance $\mathbf{P}(t)$ satisfies

$$\dot{\mathbf{\Lambda}} = -\left(\mathbf{A} - \mathbf{P}\mathbf{C}_T^T\mathbf{R}^{-1}\right)^T\mathbf{\Lambda} - \mathbf{\Lambda}\left(\mathbf{A} - \mathbf{P}\mathbf{C}_T^T\mathbf{R}^{-1}\right) - \boldsymbol{\mathcal{Q}} \tag{7}$$

with boundary condition $\mathbf{\Lambda}(t_f) = \boldsymbol{\mathcal{M}}$; and

(iii) $\mathbf{u}^*(t)$ is a solution of

$$-\boldsymbol{\mathcal{R}}\mathbf{u} = \mathbf{g}\left(\mathbf{x}\boldsymbol{\lambda}^T, \frac{\partial \mathbf{A}}{\partial \mathbf{u}}\right) + \mathbf{g}\left(\mathbf{u}\boldsymbol{\lambda}^T, \frac{\partial \mathbf{B}}{\partial \mathbf{u}}\right) + \mathbf{B}^T\boldsymbol{\lambda} + \mathbf{g}\left(\mathbf{P}(\boldsymbol{\Lambda} + \boldsymbol{\Lambda}^T), \frac{\partial \mathbf{A}_T}{\partial \mathbf{u}}\right) - \mathbf{g}\left(\mathbf{P}(\boldsymbol{\Lambda} + \boldsymbol{\Lambda}^T)\mathbf{P}\mathbf{C}_T^T\mathbf{R}^{-1}, \frac{\partial \mathbf{C}_T}{\partial \mathbf{u}}\right) + \mathbf{g}\left(\mathbf{R}^{-1}\mathbf{C}_T\mathbf{P}\boldsymbol{\Lambda}\mathbf{P}\mathbf{C}_T^T\mathbf{R}^{-1}, \frac{\partial \mathbf{R}}{\partial \mathbf{u}}\right)$$

while satisfying

$$\frac{\partial^2 H}{\partial \mathbf{u} \partial \mathbf{u}^T} \succeq 0.$$

The auxiliary function $\mathbf{g}(\mathbf{A}, \mathbf{B}) \in \mathbb{R}^{q \times 1}$ is defined as $\mathbf{g}(\mathbf{A}, \mathbf{B}) = \begin{bmatrix} \mathrm{tr}\,(\mathbf{A}\mathbf{B}_1) & \cdots & \mathrm{tr}\,(\mathbf{A}\mathbf{B}_q) \end{bmatrix}^T$ for $\mathbf{A} \in \mathbb{R}^{s \times p}$ and $\mathbf{B} = \{\mathbf{B}_1, \cdots, \mathbf{B}_q\}$ with $\mathbf{B}_i \in \mathbb{R}^{p \times s}$.

The previous result establishes necessary conditions to find the control law that minimizes the uncertainty of the estimates provided by the Kalman filter when applied to systems of the form (4). A variety of estimation problems falls under this category, for example, sensor-based simultaneous localization and mapping with measurements of range, bearing or both, source-localization, among others. The following section explores this line of thought.

## IV. Uncertainty reduction in sensor-based SLAM

Building on the results presented in the previous section, the objective of this section is to apply the uncertainty reduction control strategy of Theorem 1 to the sensor-based SLAM algorithm exposed in Section II. However, before proceeding, it is necessary to take into account that in a simultaneous localization and mapping framework not all the landmarks are visible in every instant. This means that the transformed system (2) can only be regarded as LTV (and hence used in an LTV Kalman filter) if the non-visible landmarks are discarded. Therefore, in this section, the following simplifying hypothesis is needed.

*Assumption 1:* All landmarks are always visible in the interval $[t_0, t_f]$, i.e., the set $\mathcal{M}_U$ is empty and the set $\mathcal{M}_O$ does not vary in time.

*Problem 1:* Consider the Kalman filter for the system (2). Given the matrix differential equation (6) satisfied by the error covariance of the filter with initial condition $\mathbf{P}_0$, the underlying nonlinear system (1) whose output alters the filter dynamics, the terminal time $t_f$, and the cost functional (3), determine the input $\mathbf{u}(t)$, $t_0 \leq t \leq t_f$, so as to minimize the cost functional.

The first step is to check whether the system derived in Section II fits under the category of system (4). Rewriting (1) results in a system in the form

$$\begin{cases} \dot{\mathbf{x}} = \mathbf{A}(\mathbf{u})\mathbf{x} + \mathbf{B}\mathbf{v} \\ \mathbf{y} = \mathbf{x} \end{cases} \tag{8}$$

where the state is $\mathbf{x} = \begin{bmatrix} \mathbf{b}_\omega^T & \mathbf{p}_1{}^T & \cdots & \mathbf{p}_m{}^T \end{bmatrix}$, the dynamics matrix is

$$\mathbf{A}(\mathbf{u}) = \begin{bmatrix} \mathbf{0} & \mathbf{0} \\ \mathbf{0} & \mathrm{diag}\,(-\mathbf{S}(\boldsymbol{\omega})) \end{bmatrix},$$

and the input matrix is $\mathbf{B} = \mathbf{B}_T$ as defined in Section II. Combining this information with the transformed system (2) that can be regarded as LTV, it is clear that Theorem 1 applies. This is the subject of the next result.

*Theorem 2:* Let $\mathbf{u}^*(t)$ be an admissible control which transfers $(\mathbf{x}_0, \mathbf{P}_0, t_0)$ to the target set $\mathbb{R}^{n_x} \times \mathbb{R}^{n_T \times n_T} \times \{t_f\}$. Let $\mathbf{x}^*(t)$ and $\mathbf{P}^*(t_0)$ be the trajectories of (8) and (6) corresponding to $\mathbf{u}^*(t)$, originating at $(\mathbf{x}_0, \mathbf{P}_0, t_0)$ and meeting the target set at $t_f$. In order for $\mathbf{u}^*(t)$ to be optimal for the cost functional (3), it is necessary that there exist functions $\boldsymbol{\lambda}^*(t)$ and $\boldsymbol{\Lambda}^*(t)$ such that:

(i) the vector costate $\boldsymbol{\lambda}^*(t)$ satisfies

$$\dot{\boldsymbol{\lambda}}_i = -\mathbf{S}(\boldsymbol{\omega})\boldsymbol{\lambda}_i + \sum_{j=1}^{m+1} \bar{\mathbf{S}}^T\Big(\mathbf{P}_{ij}\left(\boldsymbol{\Lambda}_{jb} + \boldsymbol{\Lambda}_{bj}^T\right)\Big) \tag{9}$$

for the bidimensional case, and

$$\dot{\boldsymbol{\lambda}}_i = -\mathbf{S}(\boldsymbol{\omega})\boldsymbol{\lambda}_i - 2\sum_{j=1}^{m+1} \mathbf{S}^{-1}\Big(\mathrm{skew}\left(\mathbf{P}_{ij}\left(\boldsymbol{\Lambda}_{jb} + \boldsymbol{\Lambda}_{bj}^T\right)\right)\Big)$$

for the tridimensional case. In both situations, the boundary condition is $\boldsymbol{\lambda}(t_f) = \mathbf{0}$;

(ii) the matrix costate $\boldsymbol{\Lambda}^*(t)$ associated with the covariance $\mathbf{P}(t)$ satisfies (7) with boundary condition $\boldsymbol{\Lambda}(t_f) = \boldsymbol{\mathcal{M}}$;

(iii) $\mathbf{u}^*(t)$ is given by

$$\begin{bmatrix} \mathbf{v}^* \\ \boldsymbol{\omega}^* \end{bmatrix} = -\boldsymbol{\mathcal{R}}^{-1} \begin{bmatrix} \mathbf{z}_v(\mathbf{x}, \mathbf{P}, \boldsymbol{\lambda}, \boldsymbol{\Lambda}) \\ \mathbf{z}_\omega(\mathbf{x}, \mathbf{P}, \boldsymbol{\lambda}, \boldsymbol{\Lambda}) \end{bmatrix} \tag{10}$$

where the part associated with the linear velocity is

$$\mathbf{z}_v = -\sum_{i=1}^{m} \boldsymbol{\lambda}_i \tag{11}$$

and that associated with the angular velocity is

$$\mathbf{z}_\omega = -\sum_{i=1}^{m} \bar{\mathbf{S}}(\mathbf{x}_i)\,\boldsymbol{\lambda}_i + 2\sum_{i=1}^{m}\sum_{j=1}^{m+1} \mathbf{S}^{-1}\Big(\mathrm{skew}\left(\mathbf{P}_{ij}\left(\boldsymbol{\Lambda}_{ji} + \boldsymbol{\Lambda}_{ij}^T\right)\right)\Big).$$

This result provides necessary conditions for the input that allows for optimal uncertainty reduction in the sensor-based SLAM problem. It achieves that by transforming the optimization problem into a two-point boundary value problem. However, solving this problem can still be complex. In optimal control problems, the forward-time costate equations are unstable, even in the linear case of the LQR. This is a major problem in shooting methods [17] that are, nevertheless relatively fast. On the other hand, the `bvp4c` method [18] is very sensitive to bad initial guesses. In this paper, the two algorithms are combined to solve the BVPs ensuing from the control problem of the current section.

*Remark 1:* Theorems 1 and 2 are derived directly from applying [11, Theorem 5-11] to the generic problem of Section III and to Problem 1. The proofs are done by tedious computation and manipulation of matrix derivatives, and are omitted due to space limitations.

## V. Simulation results and analysis

In this section, the results of solving numerically the BVP expressed by (6), (7), (8), (9), and (10) with the respective boundary conditions are presented. Several combinations of parameters are tested and their results analysed. All of

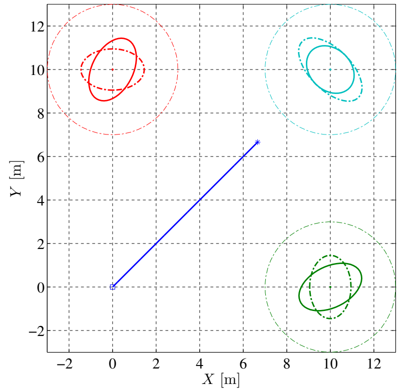


Fig. 1. The scenario of the different cases. The blue solid line is the vehicle path, the ellipsoids represent the $3\sigma$ bounds of the landmarks: the solid line is for $\mathbf{u}(t) = \mathbf{u}^*(t)$, the dashed bold line for $\mathbf{u}(t) = \mathbf{0}$, and the light dashed line is the initial covariance.

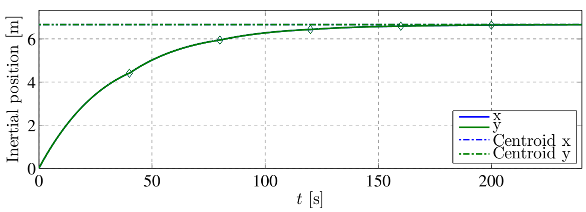


(a) Case A

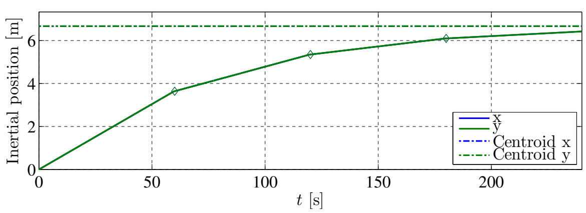


(b) Case B

Fig. 2. The trajectory of the vehicle in time for both cases. The dashed line marks the centroid of the map, and the small diamonds mark the segments in which the BVP was solved.

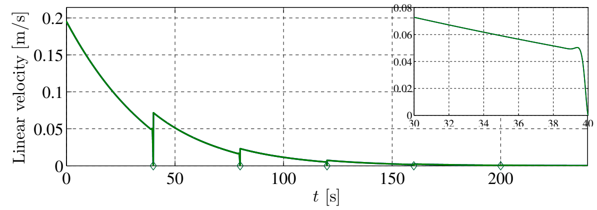


(a) Case A

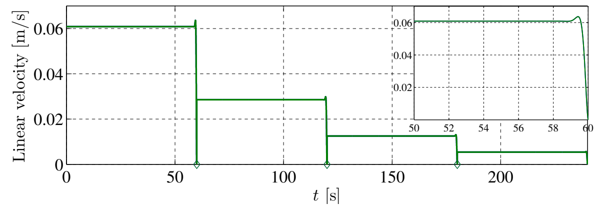


(b) Case B

Fig. 3. The input linear velocity for both cases. In the top right a close up view of the end of a segment.

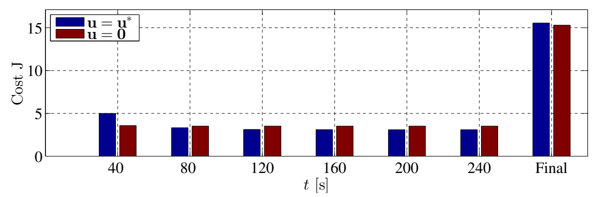


(a) Case A

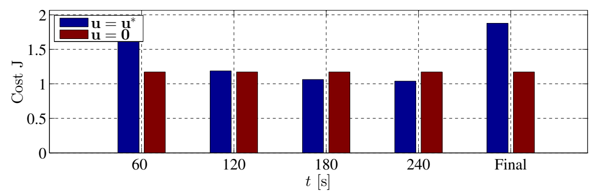


(b) Case B

Fig. 4. The cost $J(\mathbf{u})$ computed in each segment for both scenarios. The final cost is computed as if the whole simulation was a single segment.

the scenarios explored in this section are bidimensional ($n = 2$ and $\frac{1}{2}n(n-2) = 1$), and in all of them the control weight is $\boldsymbol{\mathcal{R}} = \alpha\mathbf{I}$. For better visualization and to avoid unnecessary computational problems, $m = 3$, which is enough to guarantee the convergence of the Kalman filter. Given that observability is guaranteed, the filter will converge regardless of the input. For that reason, in this section the results obtained with $\mathbf{u}(t) = \mathbf{u}^*(t)$ as given by Theorem 2 are compared with what is obtained when the vehicle does not move at all.

The main scenarios explored in this section have in common the isotropic nature of the parameters, i.e., $\mathbf{P}_0 = \mathbf{I}$, $\boldsymbol{\mathcal{M}} = \mathbf{I}$, $\mathbf{Q} = 0.1\mathbf{I}$, and $\mathbf{R} = 0.1\mathbf{I}$. The main variation is between Case A $\boldsymbol{\mathcal{Q}} \succ \mathbf{0}$; and Case B $\boldsymbol{\mathcal{Q}} = \mathbf{0}$. This change in cost functional will most likely influence the trajectory followed by the vehicle but not the steady state. The spacial configuration of both scenarios in the inertial frame is depicted in Fig. 1. There, the dark blue line represents the path of the vehicle, starting in the origin and moving towards what is seen to be the centroid of the map. The dots inside the ellipses are the landmarks, and the ellipses represent the covariance of estimation error of the filter. The large dashed ellipses are the initial condition, and the smaller bold ellipses represent the final state of $\mathbf{P}$: the solid ones are those resulting from applying $\mathbf{u}^*(t)$ to the system and the dashed ones resulting from not applying any input. Given that the steady states of both strategies are almost identical, only the overall view of Case A is shown in that figure. The main difference between the results of both scenarios is in the evolution of the position of the vehicle in time. Even though the path followed is a direct line from the origin to the map centroid for both cases, when $\boldsymbol{\mathcal{Q}} = \mathbf{0}$, the "average"covariance is not taken into account in the cost, and therefore the only intervening parts in the cost functional are the control cost and the terminal covariance cost. It is then expected that the control will take the system straight to the position that optimizes the final covariance, i.e., the centroid of the map, in contrast with the more smooth trajectory obtained when $\boldsymbol{\mathcal{Q}} \succ \mathbf{0}$. This is confirmed by the results of Fig. 2 and Fig. 3. Note that, in these cases, the attitude of the vehicle is not changed during the trajectory, as the $\boldsymbol{\omega}(t)$ input is zero. As seen in (10) and (11), when $\boldsymbol{\mathcal{R}}^{-1}$ has no components relating $\mathbf{z}_\omega$ to $\mathbf{v}(t)$, the input linear velocity is completely guided by the costate. This means that the linear

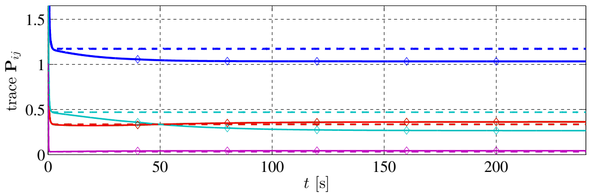


(a) Case A

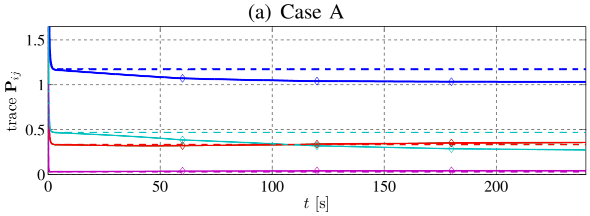


(b) Case B

Fig. 5. The evolution of the covariance $\mathbf{P}(t)$ in the different scenarios, for $\mathbf{u}^*(t)$ (solid line) and $\mathbf{u}(t) = \mathbf{0}$ (dashed). In blue is the trace of the full covariance and in violet the variance of the measurement bias estimation error. The remaining lines are $\mathrm{tr}(\mathbf{P}_i)$, $i \in \mathcal{M}$, with the colors corresponding to the landmarks in Fig. 1.

velocity in the body-fixed frame will always be zero at the end of the interval of optimization, as that is the boundary condition on the costate. This is verified by the numerical results in Fig. 3, where all the segments respect Theorem 2 independently. The necessary conditions do not guarantee optimality. In fact, when comparing the cost of applying $\mathbf{u}^*(t)$ or no input at all, depicted in Fig. 4, it can be seen that in the first segment it is a better option not to move, in the sense of minimizing $J(\mathbf{u}(t))$. In the ensuing segments this situation is inverted, even though the total cost is greater for the control strategy proposed here. However, the necessary conditions do lead towards lower uncertainty, as seen in Fig. 5, when compared to not moving. This may be due to the weight on the control being too high when compared with the terminal cost and the average covariance cost. A few other scenarios with minor variations were also approached. For example, when different size initial covariances are chosen for each landmark, the result is the same as with equal covariances. This may be related to the exponentially fast convergence of the filter. Also, when the centroid of the map is in line with the vehicle and one of the landmarks, the trajectory goes straight through the landmark. Even though this makes sense, as there is nothing in the cost functional avoiding this, it should be addressed in future work. Finally, it was observed that the time the system takes to go to the centroid of the map is greatly reduced when $\boldsymbol{\mathcal{M}}$ is increased or $\boldsymbol{\mathcal{R}}$ decreased. One of the main conclusions taken from these results is that the system tends to the centroid of the map. However, this may be due to the fact that the measurement covariance is equal for all the landmarks. In fact, a preliminary trial hinted that the vehicle tends to a point closer to the landmarks with greater $\mathbf{R}$.

## VI. Conclusions

In this paper, a novel approach to uncertainty reduction by proper motion planning is presented, grounded in the idea of optimal sensor motion planning in [2] and extended to a class of nonlinear systems where the sensor-based framework of simultaneous localization and mapping fits. Necessary conditions are found using Pontryagin's minimum principle for the optimality of the input that minimizes a cost functional that weighs the average covariance in finite horizon and the final covariance. These conditions lead to a two-point boundary value problem that can be solved numerically for horizons depending on the harshness of the optimization parameters. It is shown numerically that, when there is omnidirectional visibility of the map, this control strategy takes the vehicle to the centroid of the map.

Possible directions of future work are the inclusion of a limited field of view, the discretization of the problem, and proving the optimality of the control law.

## References


[1] M. Athans and E. Tse, "A direct derivation of the optimal linear filter using the maximum principle," *IEEE Transactions on Automatic Control*, vol. 12, no. 6, pp. 690–698, December 1967.

[2] I. I. Hussein, "Kalman filtering with optimal sensor motion planning," in *Proc. of the 2008 American Control Conference*, Seattle, Washington, USA, June 2008, pp. 3548–3553.

[3] H. Durrant-Whyte and T. Bailey, "Simultaneous Localisation and Mapping (SLAM): Part I The Essential Algorithms," *IEEE Robotics & Automation Magazine*, vol. 13, no. 2, pp. 99–110, 2006.

[4] H. J. S. Feder, J. J. Leonard, and C. M. Smith, "Adaptive mobile robot navigation and mapping," *The International Journal of Robotics Research*, vol. 18, no. 7, pp. 650–668, 1999.

[5] C. Leung, S. Huang, and G. Dissanayake, "Active SLAM using Model Predictive Control and Attractor based Exploration," in *Proc. of the 2006 IEEE/RSJ International Conference on Intelligent Robots and Systems*, Oct 2006, pp. 5026–5031.

[6] H. Carrillo, I. Reid, and J. Castellanos, "On the comparison of uncertainty criteria for active SLAM," in *Proc. of the 2012 IEEE International Conference on Robotics and Automation (ICRA)*, May 2012, pp. 2080–2087.

[7] J. Tardós, J. Neira, P. Newman, and J. Leonard, "Robust mapping and localization in indoor environments using SONAR data," *The International Journal of Robotics Research*, vol. 21, no. 4, pp. 311–330, 2002.

[8] R. Sim and N. Roy, "Global A-Optimal Robot Exploration in SLAM," in *Proc. of the 2005 IEEE International Conference on Robotics and Automation*, April 2005, pp. 661–666.

[9] L. Carlone, J. Du, M. Kaouk Ng, B. Bona, and M. Indri, "Active SLAM and Exploration with Particle Filters Using Kullback-Leibler Divergence," *Journal of Intelligent & Robotic Systems*, vol. 75, no. 2, pp. 291–311, 2014.

[10] M. Kontitsis, E. Theodorou, and E. Todorov, "Multi-robot active SLAM with relative entropy optimization," in *Proc. of the 2013 American Control Conference*, June 2013, pp. 2757–2764.

[11] M. Athans and P. Falb, *Optimal Control: An Introduction to the Theory and Its Applications*, ser. Dover Books on Engineering Series. Dover Publications, 2006.

[12] P. Lourenço, B. J. Guerreiro, P. Batista, P. Oliveira, and C. Silvestre, "Simultaneous Localization and Mapping for Aerial Vehicles: a 3-D sensor-based GAS filter," *Autonomous Robots*, 2015, accepted. [Online]. Available: http://dx.doi.org/10.1007/s10514-015-9499-z

[13] B. J. Guerreiro, P. Batista, C. Silvestre, and P. Oliveira, "Globally Asymptotically Stable Sensor-based Simultaneous Localization and Mapping," *IEEE Transactions on Robotics*, vol. 29, no. 6, pp. 1380–1395, December 2013.

[14] J. Nocedal and S. Wright, *Numerical Optimization*, 2nd ed., ser. Springer Series in Operations Research and Financial Engineering. Springer, 2006.

[15] B. D. O. Anderson, "Stability properties of Kalman-Bucy filters," *Journal of the Franklin Institute*, vol. 291, no. 2, pp. 137–144, 1971.

[16] D. Viegas, P. Batista, P. Oliveira, and C. Silvestre, "Nonlinear observability and observer design through state augmentation," in *Proc. of the 53rd IEEE Conference on Decision and Control*, Los Angeles, USA, December 2014, pp. 133–138.

[17] H. B. Keller, *Numerical Solution of Two Point Boundary Value Problems*, ser. CBMS-NSF Regional Conference Series in Applied Mathematics. Society for Industrial and Applied Mathematics, 1976.

[18] L. Shampine, M. Reichelt, and J. Kierzenka, "Solving boundary value problems for ordinary differential equations in matlab with bvp4c," October 2000. [Online]. Available: http://www.mathworks.com/bvp_tutorial